# Dirhamnolipids secreted from Pseudomonas aeruginosa modify anjpegungal susceptibility of Aspergillus fumigatus by inhibiting $\beta$1,3 glucan synthase activity.

Benoit Briard, Vero Rasoldier, Perrine Bomme, Noureddine Elaouad, Catherine Guerreiro, Pierre Chassagne, Laetitia Muszkieta, Jean-Paul Latgé, Laurence S Mulard, Anne Beauvais

OPEN

# ORIGINAL ARTICLE

# Dirhamnolipids secreted from *Pseudomonas aeruginosa* modify antifungal susceptibility of *Aspergillus fumigatus* by inhibiting β1,3 glucan synthase activity

Benoit Briard[1,5], Vero Rasoldier[1], Perrine Bomme[2], Noureddine ElAouad[3,6], Catherine Guerreiro[4], Pierre Chassagne[4,7], Laetitia Muszkieta[1,8], Jean-Paul Latgé[1], Laurence Mulard[4] and Anne Beauvais[1]

[1]*Unité des Aspergillus, Institut Pasteur, Paris, France;* [2]*Ultrapole, Institut Pasteur, Paris, France;* [3]*Fundación MEDINA, Granada, Spain and* [4]*Unité de Chimie des Biomolécules and CNRS UMR3526, Institut Pasteur, Paris, France*

***Pseudomonas aeruginosa* and *Aspergillus fumigatus* are the two microorganisms responsible for most of the chronic infections in cystic fibrosis patients. *P. aeruginosa* is known to produce quorum-sensing controlled rhamnolipids during chronic infections. Here we show that the dirhamnolipids secreted from *P. aeruginosa* (i) induce *A. fumigatus* to produce an extracellular matrix, rich in galactosaminogalactan, 1,8-dihydroxynaphthalene (DHN)- and pyo-melanin, surrounding their hyphae, which facilitates *P. aeruginosa* binding and (ii) inhibit *A. fumigatus* growth by blocking β1,3 glucan synthase (GS) activity, thus altering the cell wall architecture. *A. fumigatus* in the presence of diRhls resulted in a growth phenotype similar to that upon its treatment with antifungal echinocandins, showing multibranched hyphae and thicker cell wall rich in chitin. The diRhl structure containing two rhamnose moieties attached to fatty acyl chain is essential for the interaction with β1,3 GS; however, the site of action of diRhls on GS is different from that of echinocandins, and showed synergistic antifungal effect with azoles.***
*The ISME Journal* (2017) **11,** 1578–1591; doi:10.1038/ismej.2017.32; published online 24 March 2017

## Introduction

*Aspergillus fumigatus* and *Pseudomonas aeruginosa* are the two microorganisms responsible for most of the chronic infections encountered in cystic fibrosis adult patients. *A. fumigatus* is indeed the major filamentous fungus reported to colonize the airways of these patients, with a prevalence of 12–57% (Paugam *et al.*, 2010), and major risks in developing allergic bronchopulmonary aspergillosis in 15% of patients (Knutsen *et al.*, 2012; Baxter *et al.*, 2013). The most common bacterium isolated from the sputum of patients with cystic fibrosis is *P. aeruginosa*, which chronically colonizes cystic fibrosis airways in up to 75% of adult patients (Hill *et al.*,

2005; Moree *et al.*, 2012; Baxter *et al.*, 2013). The co-colonization by *A. fumigatus* and *P. aeruginosa* is very deleterious for the patients, characterized by a high decline in cystic fibrosis pulmonary functions and the worst prognosis with no access to lung transplantations (Ferreira *et al.*, 2015).

Several recent studies have shown that *P. aeruginosa* and *A. fumigatus* interact during lung colonization. The first evidence for crosstalk's *in vivo* between *A. fumigatus* and *P. aeruginosa* emerged from the fact that antibacterial therapy targeting *P. aeruginosa* colonization is followed by a significant reduction in *A. fumigatus* colonization (Baxter *et al.*, 2013). Two studies have shown a direct interaction between *P. aeruginosa* and *A. fumigatus* (Blyth, 1971; Mowat *et al.*, 2010). *P. aeruginosa* secretes molecules such as homoserine-lactones, phenazines, siderophores, quinolones, which interfere with the behavior of *A. fumigatus* (Mowat *et al.*, 2010; Moree *et al.*, 2012; Briard *et al.*, 2015). Homoserine-lactones reduce the growth of *A. fumigatus*, whereas phenazines have a dual effect on *A. fumigatus*. At low concentrations such as in an iron-starved environment, pyocyanin, phenazine-carboxamide and phenazine-carboxylic acid could

stimulate the growth of *A. fumigatus* by reducing the Fe(III). However, at high concentrations, all phenazines (including 1-hydroxy-phenazine) penetrated into the cells and induced the production of reactive-oxygen species and reactive-nitrogen species leading to fungal death (Briard *et al.*, 2015). Such interactions were not demonstrated *in vivo*; however, phenazines were detected in the sputum of cystic fibrosis patients at concentrations which stimulated the growth of *A. fumigatus in vitro* (Wilson *et al.*, 1988; Bjarnsholt *et al.*, 2010; Briard *et al.*, 2015). Regarding quinolones, their effect on *A. fumigatus* or on other fungi was never studied (Diggle *et al.*, 2003).

The present study is centered on rhamnolipids (Rhls), which are secreted by *P. aeruginosa* and other *Pseudomonas* species (Abalos *et al.*, 2001; Moree *et al.*, 2012). To date these molecules have been shown to display only tension active properties. Our study demonstrated that the growth inhibition of *A. fumigatus* and an increased thickness of *A. fumigatus* cell wall following the adhesion of *P. aeruginosa* to *A. fumigatus* is due to the secretion of dirhamnolipids (diRhls) which inhibit the fungal β1,3 glucan synthase (GS).

## Materials and methods

### Strains and culture conditions
The *A. fumigatus* reference strain used in this study is CEA17ΔakuB$^{KU80}$ (ku80) deficient in non-homologous end joining (da Silva Ferreira *et al.*, 2006), which originates from the clinical isolate CBS 144-89, and is as pathogenic as CBS 144-89 in experimental murine aspergillosis models.

CEA17ΔakuB$^{KU80}$ was used to generate the Δ*pksP*, Δ*hppD*, Δ*sph3* deletion strains and EMFR S678P mutant. Δ*pksP* is a 1,8-dihydroxynaphthalene (DHN)-melanin-deficient mutant (Jahn *et al.*, 2000); Δ*hppD* is a pyo-melanin-deficient mutant and is a kind gift of AA Brakhage (Hans Knöll Institute, Jena, Germany) (Schmaler-Ripcke *et al.*, 2009); Δ*sph3* is a spherulin-4-like-deleted mutant, deficient in the production of galactosaminogalactan (GAG), constructed as described in the Supplementary Information (Supplementary Figure 1). EMFR S678P is resistant to caspofungin, due to a point mutation for Serine$^{678}$ in proline in the unique *FKS* gene coding for the β1,3 GS (Rocha *et al.*, 2007), and is a kind gift from DS Perlin (Public Health Research Institute, Newark, NJ, USA).

All strains were conserved on 2% (w/v) malt agar slants. One-week-old conidia were recovered from the slants by vortexing with 0.05% (v/v) aqueous Tween 20 solution and used for inoculation in 2YT or Minimal Medium (Briard *et al.*, 2015), RPMI (Clavaud *et al.*, 2012) or Sabouraud (Lamarre *et al.*, 2009) media.

The *P. aeruginosa* used in this study is the reference strain PAO1 (Holloway *et al.*, 1994). This strain was used to generate the deletion strain, Δ*rhlA*, which do not produce Rhls and is a kind gift

of Niels Høiby (Department of clinical microbiology, Rigshospitalet, Copenhagen) (Jensen *et al.*, 2007). *P. aeruginosa* strains were conserved in 2YT medium containing 50% glycerol at − 80 °C.

### Co-culture of A. fumigatus and P. aeruginosa
To determine the best conditions, preliminary experiments were done with different culture agar-media in Petri dishes (90 mm diameter) as described in the Supplementary Information. The selected co-interaction model is $2 \times 10^7$ ku80 conidia inoculated on RPMI plates spotted at the same time with 5 µl of $2.5 \times 10^5$ PAO1 and incubated for 16 h at 37 °C.

### Culture of A. fumigatus in presence of culture filtrate or dirhamnolipids of P. aeruginosa
PAO1 ($A_{600} = 0.05$) was inoculated in 50 ml 2YT for 24 h at 37 °C. The bacteria were separated by centrifugation at 15 000 r.p.m. for 10 min and the culture filtrate (CF) was filtrated through 0.22 µm Minisart filter (Sigma-Aldrich, Saint-Quentin Fallavier, France). *A. fumigatus* conidia ($2 \times 10^7$) suspended in 3 ml 0.4% agar containing PAO1 CF was overlaid on RPMI-agar and incubated for 16 h at 37 °C. The mycelia grown were observed by transmission electron microscopy (TEM) as described below.

To screen for the CF-active fraction during purification (described below), $1.5 \times 10^4$ *A. fumigatus* conidia ml$^{-1}$ were inoculated on eight-well glass bottom Ibidi µ-slides in 2YT medium reconstituted using the PAO1 CF instead of water or in presence of purified diRhls (obtained from CF as described below). The culture was incubated at 37 °C for 24 h. Mycelium was observed under light microscopy.

### Analysis of the binding of P. aeruginosa to A. fumigatus polysaccharides, melanin and hyphae
*P. aeruginosa* was incubated with *A. fumigatus* cell wall α1,3 glucan, β1,3 glucan, galactomannan, GAG, melanin, chitin (Sigma-Aldrich), and ku80 or Δ*sph3* hyphae as described in the Supplementary Information.

### Scanning and transmission electron microscopy preparation
The zone of partial fungal–bacterial inhibition (Figure 1a) from *A. fumigatus* and *P. aeruginosa* co-culture was cut in the Durapore filter, fixed in 2.5% glutaraldehyde in 0.1 M sodium cacodylate buffer for 24 h at 4 °C and prepared for scanning electron microscopy and TEM (Lamarre *et al.*, 2009; Briard *et al.*, 2015). As a control, the same culture was prepared without *P. aeruginosa*.

The thickness of the cell wall was calculated from 50 hyphae with six measures per hyphae from TEM pictures using the ImageJ/fiji analysis (Schneider *et al*, 2012).
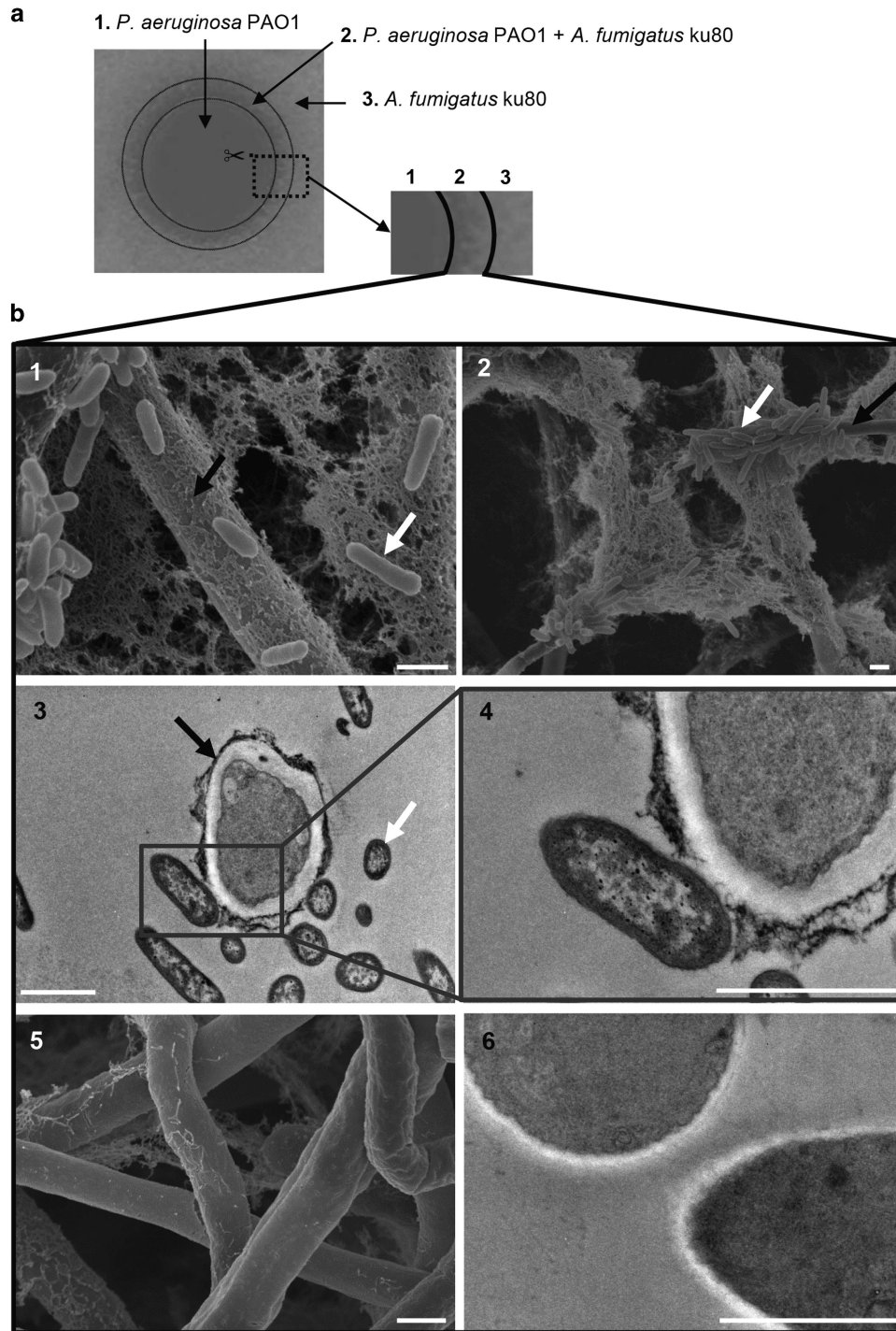
**Figure 1** Interaction between *A. fumigatus* ku80 and *P. aeruginosa* PAO1 strains. (**a**) Zone of partial inhibition (dotted square) between *A. fumigatus* and *P. aeruginosa*. (**b**) Scanning (**b1**, **2** and **5**) and transmission (**b3**, **4** and **6**) electron microscopy views of the zone of partial inhibition; (**b1–4**) ku80-PAO1; (**b4**) enlargement of the interaction zone showed in **b3**; (**b5** and **6**) control ku80 in the absence of PAO1. White arrow, bacteria; black arrow, fungus. Note the presence of an increased amount of fungal ECM in presence of *P. aeruginosa* (**b1** compared to **b5** and **b3** compared to **b6**). Scale bars, 1 µm.

*Extraction and isolation of the active molecules from*
P. aeruginosa *24 h culture filtrate*
The PAO1 24 h CF was extracted twice with ethyl acetate (1:1) and the organic phase was evaporated and dried. A mixed fraction, F-diRhls, containing two to three diRhls depending on the CF batches, was purified from the organic extract as described in the Supplementary Information. Each fraction was identified by high-resolution mass spectrometry, which correlated with the published data (Sharma *et al.*, 2007; Abdel-Mawgoud *et al.*, 2010; Arutchelvi and Doble, 2010).
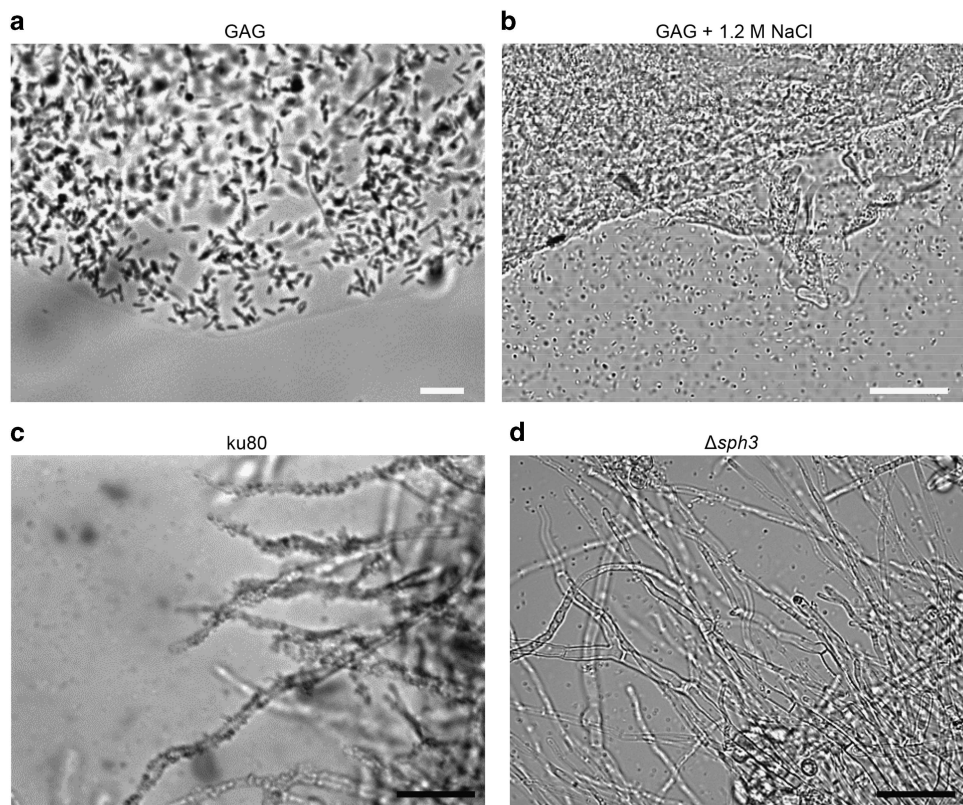
**Figure 2** Binding of *P. aeruginosa* to *A. fumigatus* GAG. (**a**) incubation of PAO1 with purified GAG. (**b**) Incubation of PAO1 with purified GAG in presence of 1.2 M NaCl. (**c**) Adhesion of PAO1 to *A. fumigatus* ku80 hyphae. (**d**) Absence of adhesion of PAO1 to *AfΔsph3* mutant hyphae, unable to produce GAG. Note that the binding of PAO1 to GAG is inhibited under high salt concentration (**b**). Scale bars, 25 μm.

*Chemical synthesis of dirhamnolipid analogs diRhamnose-C₃ and diRhamnose-C₈*

The synthesis of two diRhls analogs, diRhamnose-$C_3$ (diRha-$C_3$) and diRhamnose-$C_8$ (diRha-$C_8$) bearing a simpler aglycon—a propyl and an octyl chains, respectively, is described in the Supplementary Information.

*Method for susceptibility testing and biomass quantification by crystal violet*

Minimal effective concentration (MEC) of the molecules was determined according to the Clinical Laboratory Standards Institute M38-A2 protocol (NCCM) by microdilution method in 96-well plates using crystal violet biomass quantification as previously described (Briard *et al.*, 2015).

*Determination of the fractional inhibitory concentration (FIC) index (FICi)*

The FICi of drug interactions was determined via checkerboard titration assays (Clavaud *et al.*, 2012). The concentrations of the antifungal agents ranged from 0.008 to 1 μg ml$^{-1}$, 0.004 to 0.5 μg ml$^{-1}$ and 0.031 to 4 μg ml$^{-1}$ for caspofungin, voriconazole and itraconazole, respectively. The concentrations of F-diRhls ranged from 0.03 to 4 mM. Serial twofold dilutions of antifungals were prepared with the assay culture in 2YT in 96-wells flat bottom plates as

described above. The microtiter plates were incubated at 37 °C for 20 h and the growth biomass was assessed using crystal violet and resazurin methods (Clavaud *et al.*, 2012; Briard *et al.*, 2015). The pharmacodynamic interaction analysis was done as described (Mavridou *et al.*, 2015). Briefly, the synergistic, additive or antagonistic effect of paired combinations of drugs was captured by the FICi: (a) $FIC = FIC_{drugA} + FIC_{drugB}$; (b) $FIC_{drugA} = MIC_{drugsA+B}/MIC_{drugA}$; and (c) $FIC_{drugB} = MIC_{drugsA+B}/MIC_{drugB}$. If the FIC $\Sigma FICmin$ value is lower than 1, this indicates synergistic interactions between two drugs; if FIC $\Sigma FICmax$ value is higher than 1.25, then an antagonistic interaction exists and between these two values, the interactions between the two drugs are additive.

*Effect of diRhl on cell wall*

Glucosamine and galactosamine determination in ku80 cell wall in presence and absence of F-diRhls and preparation of cell-free glucan and chitin synthases extracts are described in the Supplementary Information.

*Statistical analysis*

Data are reported as means ± s.e.m. Comparisons, performed with Graph Pad Prism 3.0 software (http://graphpad-prism.software.informer.com/3.0/) and analysis of variance statistical test.
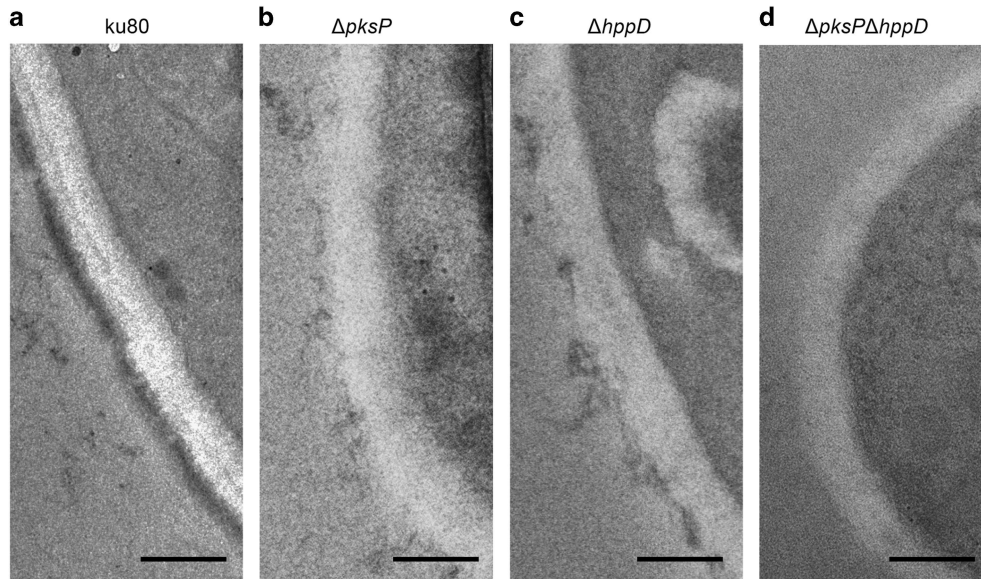
**Figure 3** Presence of melanin in the ECM of *A. fumigatus* ku80 during co-cultivation with *P. aeruginosa* PAO1 in RPMI. (**a**) Parental strain ku80. (**b**) *Af*Δ*pksP* mutant unable to produce DHN-melanin. (**c**) *Af*Δ*hppD* mutant unable to produce pyo-melanin. (**d**) Double *Af*Δ*pksP*Δ*hppD* mutant. Note the absence of melanin in *Af*Δ*pksP*Δ*hppD*, showing that melanin in ECM is a mixture of DHN and pyo-melanin. Scale bars, 250 nm.

## Results

*Morphological modifications of* A. fumigatus *mycelium in presence of* P. aeruginosa

Preliminary experiments determined the best culture conditions allowing the fungus and the bacterium to grow together: $2 \times 10^7$ ku80 *A. fumigatus* conidia were inoculated on an RPMI agar plates and at the same time 5 µl of $2.5 \times 10^5$ PAO1 *P. aeruginosa* was spotted in the center of the Petri-dish. Under these experimental conditions, a zone of partial fungal inhibition was observed at the junction between the bacterial and the fungal colonies (Figure 1a). The zone of partial inhibition was observed under scanning electron microscopy and TEM (Figure 1b). The first observation under scanning electron microscopy showed an electron-dense extracellular matrix (ECM) embedding the hyphae of *A. fumigatus* which was more abundant in the presence of the bacteria than in its absence (Figures 1b1, b2 and b5). PAO1 cells adhered to the hyphae, mainly at their apex and to the ECM (Figures 1b1, b2). To identify the fungal cell wall molecule to which *P. aeruginosa* was binding, the *A. fumigatus* cell wall polysaccharides α1,3 glucan, β1,3 glucan, galactomannan, chitin, GAG and melanin (Latgé, 2010) were incubated with the PAO1 cells and scored the binding under light microscopy. The bacteria only bound to GAG (Figure 2; Supplementary Figure 2 and data not shown). Addition of 1.2 M NaCl prevented the binding of the bacteria to GAG showing that PAO1 binding was due to ionic interactions (Figures 2a and b). To confirm that GAG is responsible for the binding of *P. aeruginosa* to *A. fumigatus* ku80 hyphae, the spherulin-4 like gene, coding for Sph3 involved in the synthesis of GAG in *A. fumigatus*

(Bamford *et al.*, 2015) was deleted in ku80 (Supplementary Figure 1) and the Δ*sph3* strain was incubated with *P. aeruginosa*. As shown in Figures 2c and d, *P. aeruginosa* did not bind to Δ*sph3* hyphae.

The interaction between bacterium and fungus induced formation of an electron-dense ECM around the fungal hyphae. This electron-dense material was absent in the control cultures (in absence of bacteria) as well as at the contact point between the fungal cell wall and *P. aeruginosa* PAO1 (Figures 1b3). This electron-dense material is reminiscent of melanin observed around hyphae in the *A. fumigatus* biofilm (Beauvais *et al.*, 2007). Three *A. fumigatus* deletion mutants Δ*pksP*, Δ*hppD* and Δ*pksP*Δ*hppD* affected in DHN-, pyo- or both melanin synthesis, respectively (Jahn *et al.*, 2000; Schmaler-Ripcke *et al.*, 2009), were grown in with the presence of PAO1. As shown in the Figure 3, this electron-dense material was partially lost in Δ*pksP* and Δ*hppD*, and was absent in Δ*pksP*Δ*hppD*. Therefore, the electron-dense material present in the ECM in presence of PAO1 was composed of both DHN- and pyo-melanin.

TEM also showed that *A. fumigatus* presented a thicker cell wall (104 nm ± 3.2) when grown in the presence of *P. aeruginosa* (Supplementary Figure 3), compared to that in its absence (72 nm ± 1.19). This observation suggested that bacterial co-culture induced modification of the fungal cell wall structure.

P. aeruginosa *secreted dirhamnolipids are responsible for the* A. fumigatus *cell wall modification*

To test whether *P. aeruginosa* induced cell wall modifications in *A. fumigatus* requires its direct
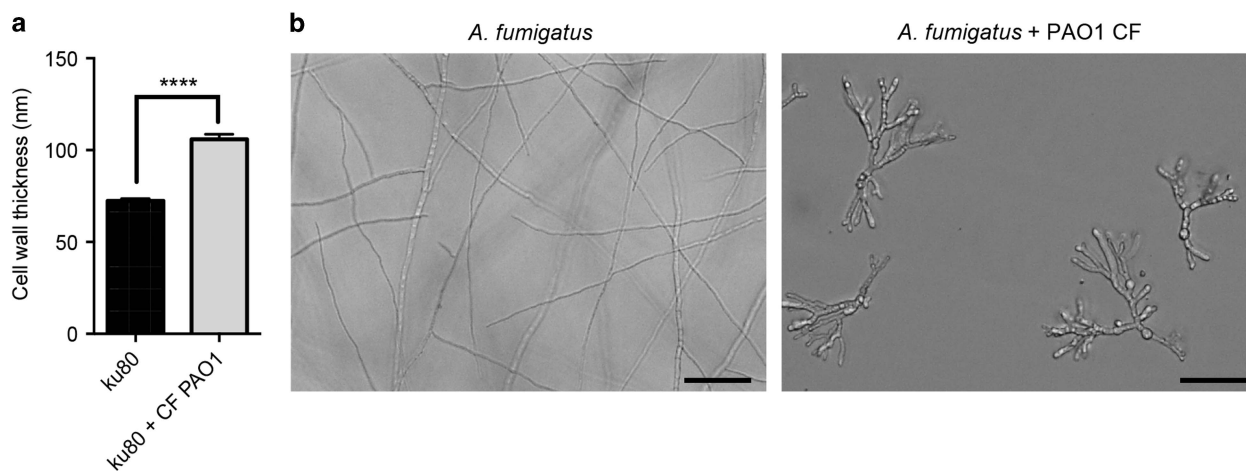
**a**



**b**

| *A. fumigatus* | *A. fumigatus* + PAO1 CF |



**Figure 4** *A. fumigatus* hyphal morphology grown in presence of 24 h PAO1 CF. (**a**) Thickness of *A. fumigatus* ku80 cell wall in presence of CF in RPMI, calculated from 50 hyphae with six measures per hyphae from TEM pictures using the ImageJ/fiji analysis (Schneider et al, 2012). (**b**) Light microscopy images showing the increased branching of the fungal hyphae in presence of CF. Scale bar 50 μm.

**a**



diRha-$C_{10}$-$C_{10}$
$t_R$: 7.29 min

($C_{32}H_{58}O_{13}$)
650.39 g.mol$^{-1}$

**b**



diRha-$C_{10}$-$C_{11}$
$t_R$: 8.93 min

($C_{33}H_{59}O_{13}$)
664.4 g.mol$^{-1}$

**c**



diRha-$C_{10}$-$C_{12:1}$
diRha-$C_{12:1}$-$C_{10}$
$t_{R1}$: 9.10 min
$t_{R2}$: 9.47 min

($C_{34}H_{60}O_{13}$)
676.4 g.mol$^{-1}$
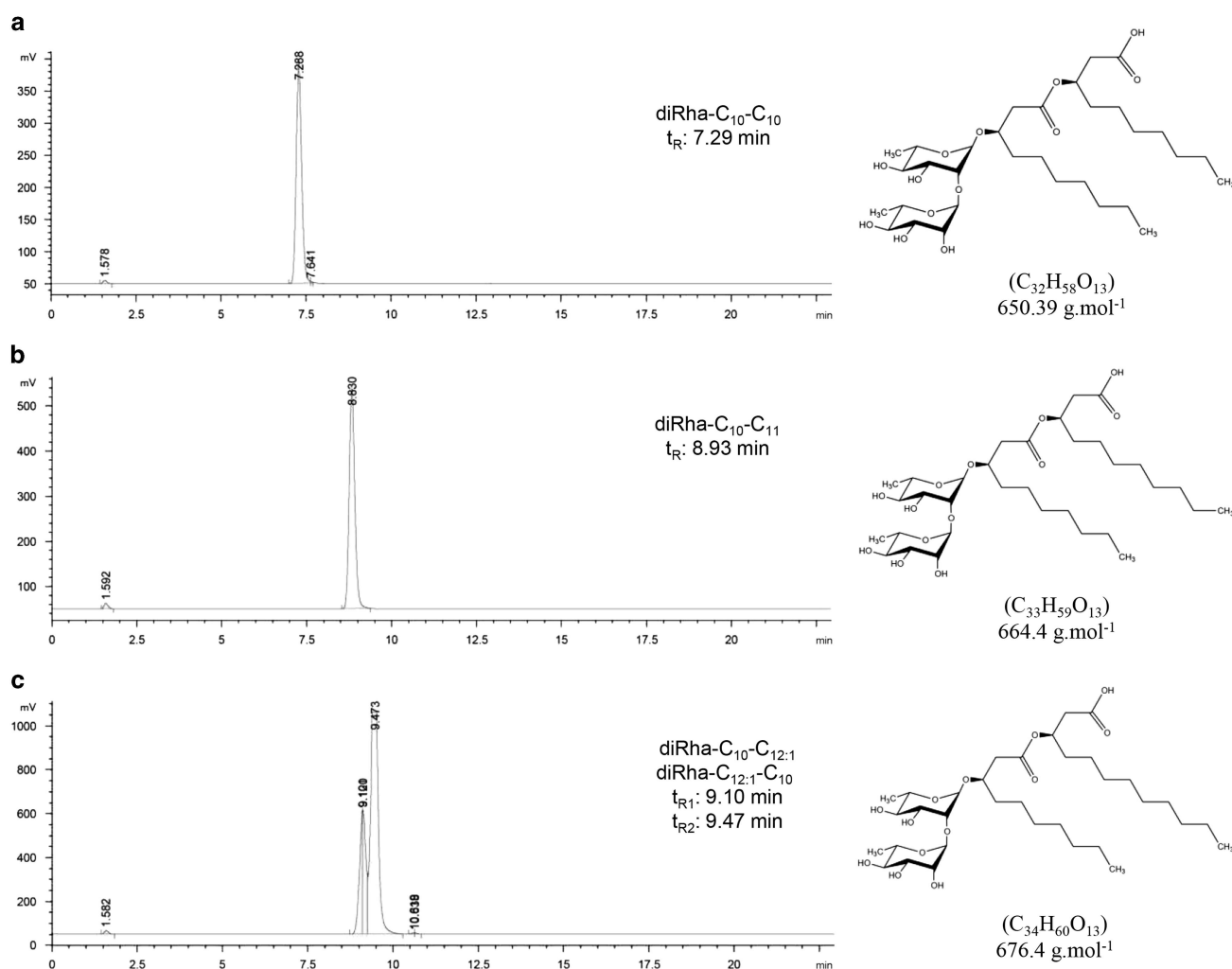
**Figure 5** Analytical RP-HPLC profiles of the dirhamnolipids isolated following RP-HPLC purification of the 24 h culture filtrate of *P. aeruginosa*. Elution from a C18 Kromasil column (4.6 × 150 mm, 5 μm, 100 Å) at 1.0 ml min$^{-1}$ with $CH_3CN$ in 0.08% aqueous trifluoroacetic acid (60 → 100% over 15 min.), detection with an evaporative light scattering detector and identification according to the literature (Sharma *et al.*, 2007; Abdel-Mawgoud *et al.*, 2010; Arutchelvi and Doble, 2010). (**a**) diRha-$C_{10}$-$C_{10}$. (**b**) diRha-$C_{10}$-$C_{10}$-$CH_3$ (diRha-$C_{10}$-$C_{11}$) corresponding to the methyl ester of diRha-$C_{10}$-$C_{10}$. (**c**) diRha-$C_{10}$-$C_{12:1}$ and diRha-$C_{12:1}$-$C_{10}$ bearing an unsaturated fatty acid.

contact or due to molecules secreted from bacteria, *A. fumigatus* conidia were incubated in the presence of bacterial CF. The CF from either 2YT or RPMI media promoted the formation of an ECM around fungal hyphae and induced thickening of the fungal cell wall (Figure 4a). Increase in the fungal cell wall thickness (106 nm) was comparable to that observed when bacteria are directly in contact with the fungus. In addition, *A. fumigatus* growth was reduced with multibranched hyphae, the phenotype similar when this fungus is grown in the presence of antifungal echinocandins (Figure 4b; Perlin, 2011).

These results suggested that diffusible molecules in *P. aeruginosa* PAO1 CF were responsible for the fungal cell wall modifications.

The molecules responsible for the cell wall phenotype were then purified from a 2YT CF of *P. aeruginosa* after 24 h of growth. Only one high-performance liquid chromatography fraction gave the cell wall phenotype mentioned above when incubated with *A. fumigatus*. MS analyses (data not shown) showed that this fraction contained a mixture of diRhls (F-diRhls). Following purification, three rhamnobiosides differing by the length of their
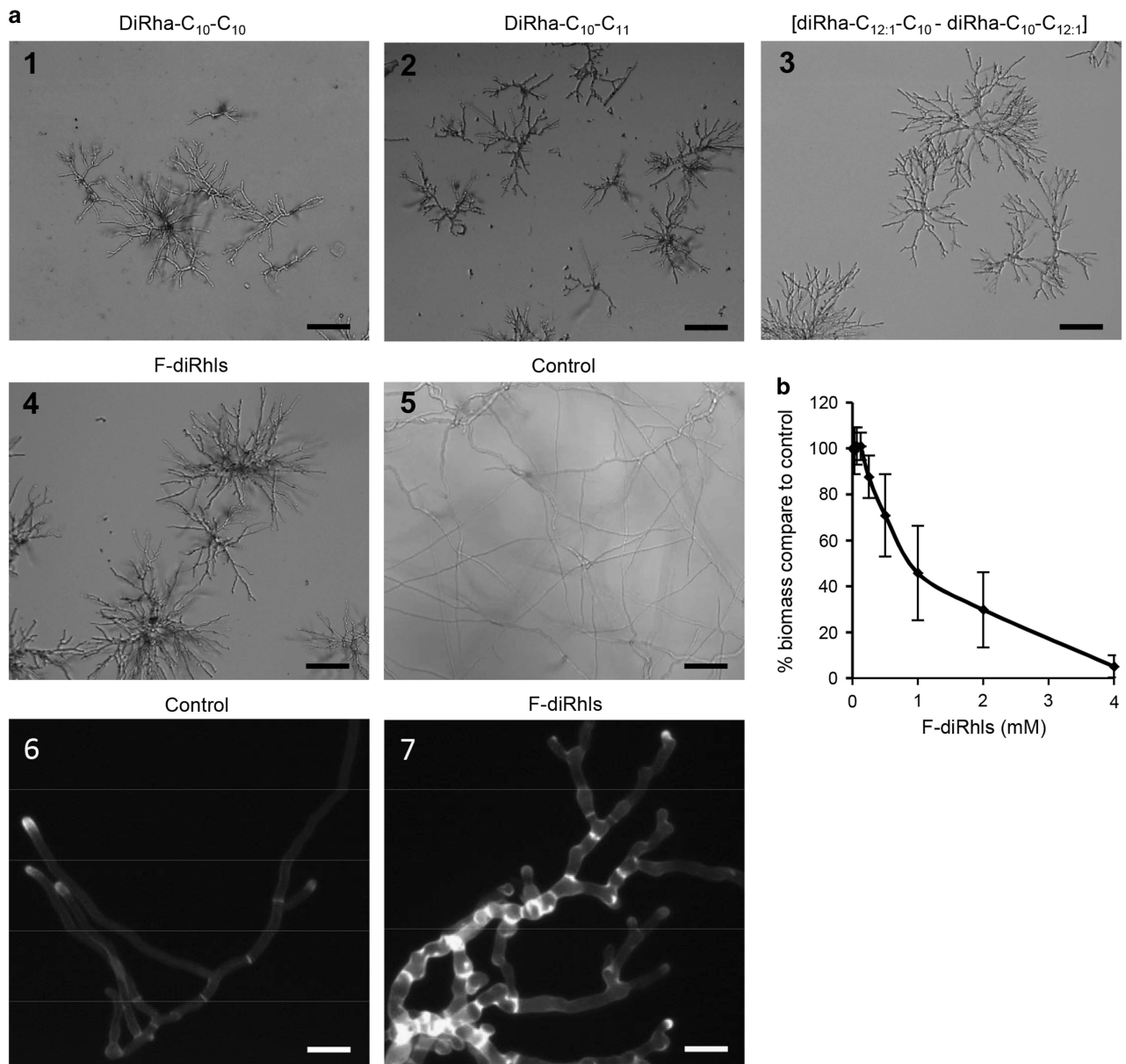


**Figure 6** Impact of the diRhls on the *A. fumigatus* mycelial growth. (**a1–4**) Light microscopy of *A. fumigatus* grown for 24 h in the presence of diRha-$C_{10}$-$C_{10}$, diRha-$C_{10}$-$C_{11}$, [diRha-$C_{12:1}$-$C_{10}$ - diRha-$C_{10}$-$C_{12:1}$] or F-diRhls at 4 mM. (**a5**) *A. fumigatus* grown in the absence of diRhls. Note the increased branching of mycelium after growth with diRhls. (**a6** and **7**) UV microscopy of calcofluor white labeling of *A. fumigatus* in the absence or presence of diRhls. Note the increased amount of fluorescence in the hyphae in presence of F-diRhls, which is representative of an increase in the chitin. (**b**) Reduction of mycelial growth by different concentrations of F-diRhls. Scale bars, 50 µm (**a1–a5**); 10 µm (**a6** and **a7**).

fatty acid chains were identified: diRha-$C_{10}$-$C_{10}$ eluting at $t_R$: 7.29 min had *m/z* 650.39 (HRMS-ESI⁺ for $C_{32}H_{58}O_{13}$ ([M+Na]⁺, 673.3775), diRha-$C_{10}$-$C_{11}$ eluting at $t_R$: 8.93 min had *m/z* 664.4 (HRMS-ESI⁺ for $C_{33}H_{60}O_{13}$ ([M+Na]⁺, 687.3932), diRha-$C_{10}$-$C_{12:1}$ and diRha-$C_{12:1}$-$C_{10}$ eluting at $t_R$: 9.10 min and 9.47 min, respectively, had *m/z* 676.4 (HRMS-ESI⁺ for $C_{34}H_{60}O_{13}$ ([M+Na]⁺, 699.3932) (Figure 5). F-diRhls was majorly composed of diRha-$C_{10}$-$C_{10}$ (60–100% depending of the CF batches). Each diRhls was either tested individually or in combination (F-diRhls) on *A. fumigatus.*

TEM observation of the hyphae after treatment with 4 mM diRha-$C_{10}$-$C_{10}$ showed an increased thickness of the cell wall (215 nm ± 5,6) and ECM as observed previously with *P. aeruginosa* PAO1 and its CF (Supplementary Figures 4a and c). This increased thickness of the cell wall could be correlated to an increased concentration of the GAG adhesin at the cell surface. This hypothesis was verified biochemically by determination of the amount of galactosamine monomers, representative of GAG, in the extracted cell wall in absence and presence of 4 mM F-diRhls; 1.74 µg (± 0.44)

galactosamine per mg mycelium dry weight was found in *A. fumigatus* cell wall in the absence of F-diRhls which was significantly increased to 11.26 µg (±0.14) galactosamine per mg mycelium dry weight in the presence of F-diRhls.

To confirm that F-diRhls were responsible for the morphological changes in *A. fumigatus* cell wall, co-culturing of the fungus and the *P. aeruginosa* Δ*rhlA* mutant, which is unable to synthesize Rhls, was undertaken. The Δ*rhlA* mutant bound to ku80 hyphae similar to *P. aeruginosa* PAO1 but no melanin was present as in the control without bacteria (Figure 1b6; Supplementary Figure 4b). Moreover, the cell wall thickness was not modified in presence of Δ*rhlA* (Supplementary Figure 4c). These results confirmed that the cell wall phenotype induced by the bacterium was due to the presence of diRhls secreted by PAO1.

### Fungal growth phenotype is due to the inhibition of β1,3 glucan synthase by diRhls

*A. fumigatus* had a reduced growth and altered morphology in presence of diRhls similar to that
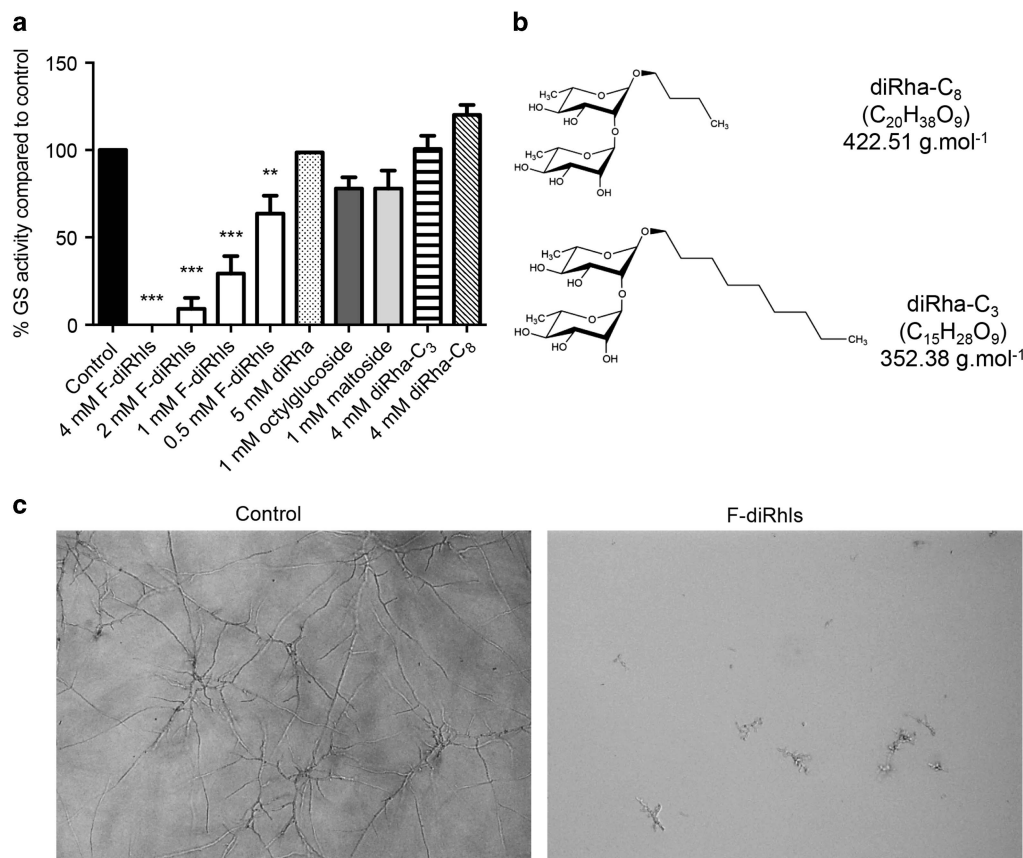


**Figure 7** Specific inhibition of *A. fumigatus* ku80 β1,3 glucan synthase activity by dirhamnolipids (F-diRhls). (**a**) β1,3 glucan synthase activity (**$P = 0.0036$; ***$P < 0.0001$); 0.5–4 mM F-diRhls, 5 mM rhamnobiose (diRha), 1 mM octylglucoside and maltoside, 4 mM propyl- and octyl-rhamnobioside analogs (diRha-C3 and diRha-C8, respectively) were added in the glucan synthase reaction mixture ($P > 0.05$). (**b**) Structure of the chemically synthesized diRha-$C_3$ and diRha-$C_8$. (**c**) phenotype of *A. fumigatus* EMFR S678P in absence and presence of 0.5 mM F-diRhls.

observed with CF (Figures 4b and 6a). The effect of F-diRhls on *A. fumigatus* was never fungicidal whatever concentration used. The short hyperbranched morphology was reminiscent of the echinocandin effect. Accordingly, only an MEC, which is the lowest drug concentration resulting in aberrant hyphal growth, can be measured (Arikan *et al.*, 2002). The MEC was 4 mM, and resulted in 90% inhibition of *A. fumigatus* growth (Figure 6b). Calcofluor white treatment showed an increase in hyphal fluorescence compared to untreated control after treatment with purified diRhls and F-diRhls at MEC, suggesting an increase in the concentration of cell wall chitin (Figures 6a6 and 7). This hypothesis was verified biochemically by determination of the amount of glucosamine monomers, representative of chitin, in the extracted cell wall treated and untreated with F-diRhls at MEC; in the absence of F-diRhls, 9.15 µg (± 1.55) glucosamine per mg mycelium dry weight was found, which was significantly increased (31.4 µg (± 0.38) glucosamine per mg mycelium dry weight) in the presence of F-diRhls. An increase in the cell wall chitin amount was also observed after incubation of the fungus with echinocandins (Walker *et al.*, 2010). These data suggested that diRhls may have a direct effect on the $\beta$1,3 GS activity. Indeed, the F-diRhls inhibited the GS activity in a dose–response manner (Figure 7a). To determine if the inhibition of the GS activity was due to the detergent characteristic of the F-diRhls, other neutral nonionic detergent glycolipids such as octylglucoside and maltoside were tested. These detergents disrupt protein–lipid and lipid–lipid interactions in the membrane, which could disturb their activity. Figure 7a showed a slight statistically insignificant inhibition of GS activity by octylglucoside and maltoside, showing that the dose-dependent inhibition of GS by F-diRhs was mainly due to their GS-specific effect. Moreover, we verified the specificity of F-diRhls on the GS activity by testing the chitin synthase activity in presence of 1 mM F-diRhls, octylglucoside and maltoside. All compounds induced a similar statistically insignificant decrease of the chitin synthase activity (Supplementary Figure 5), showing that in contrast to GS inhibition, their minimal effect on the chitin synthase was not specific, and was due to biosurfactant activity on the membranes.

To investigate the active moiety of F-diRhls on GS activity, we tested the inhibitory effect of rhamnobiose and the propyl- and octyl-rhamnobioside analogs, equipped with a linear three carbons (diRha-C$_3$) and eight carbons (diRha-C$_8$) aglycon (Figures 7a and b). None of these molecules inhibited GS activity, suggesting that the branched lipidic tail with $\beta$-hydroxy fatty acids of F-diRhls is essential for its activity against GS.

The *A. fumigatus* EMFR S678P strain, which is a mutant resistant to caspofungin consecutively to a point mutation in the binding site of this echinocandin to GS, has a MEC $\geqslant$16 µg caspofungin ml$^{-1}$, while the MEC of caspofungin for parental ku80 strain is 0.25 µg ml$^{-1}$ (Rocha *et al.*, 2007).

**Table 1** Pharmacodynamic interaction concentration index (FICi) between F-diRhls and CAS, ITR or VTR for *A. fumigatus* ku80

| | MEC[a] or MIC[b] drugs alone | | | MEC or MIC drugs in combination | | | $\sum$FICmin, $\sum$FICmax index[c] | | |
|---|---|---|---|---|---|---|---|---|---|
| F-diRhls (mM) | CAS (µg ml$^{-1}$) | ITR (µg ml$^{-1}$) | VRC (µg ml$^{-1}$) | F-diRhls, CAS | F-diRhls, ITR | F-diRhls, VRC | F-diRhls, CAS | F-diRhls, ITR | F-diRhls, VRC |
| 4 | 0.25 | 16 | 0.3 | 1, 1 | 2, 1 | 1, 0.063 | 2.2, 4.25 | 0.56, 0.5 | 0.5, 0.56 |

Abbreviations: CAS, caspofungin; diRhls, dirhamnolipids; ITR, itraconazole; MEC, minimal effective concentration; VTR, voriconazole.
[a]MEC for F-diRhls and CAS.
[b]MIC for itraconazole and voriconazole.
[c]FICi $\sum$FICmin <1 = synergy; FICi $\sum$FICmax >1.25 = antagonism; 1< FIC <1.25 = additive.

Surprisingly, the MEC of F-diRhls on the EMFR S678P strain was 0.5 mM compared to the 4 mM value with the *A. fumigatus* ku80 strain (Figure 7c). This result indicated that the diRhls and the echinocandin do not bind to the same GS site and that the S678P mutation favored the inhibitory effect of F-diRhls towards GS activity. When F-diRhls and caspofungin were tested in combination on the ku80 strain, the combined effect of two molecules was antagonist with a FICi ΣFICmax of 4.25 (Table 1). In contrast to the previously reported additive effect of caspofungin with voriconazole (Elefanti *et al.*, 2013), the results presented in Table 1 showed that the combined effect of F-diRhls and voriconazole or itraconazole was synergistic with a FICi ΣFICmin of 0.5 and 0.56, respectively. These data supported the fact that diRhls and caspofungin target the same component of *A. fumigatus*, the GS.

This study shows that the F-diRhls induce several morphological effects: (i) they modify the nature of fungal ECM surrounding the *A. fumigatus* hyphae; (ii) they inhibit the growth of *A. fumigatus* and induce the formation of short multibranched hyphae, which results from the specific inhibition of the fungal GS activity; (iii) they induce a thickening of the cell wall due to compensatory reactions resulting from an increased chitin concentration to palliate the antifungal effect of dirhamnolipids; and (iv) the site of action of diRhls on GS is different from that of echinocandins, which facilitates its synergistic activity with azoles.

## Discussion

This study has shown that *P. aeruginosa* binds strongly to the *A. fumigatus* hyphae. We previously reported that the polysaccharides composing *A. fumigatus* ECM were α1,3 glucan, GAG and galactomannan (Beauvais *et al.*, 2007). In the binding experiments, in presence of *P. aeruginosa*, only GAG was found to be the molecule responsible for *P. aeruginosa* to *A. fumigatus* binding. GAG has been reported previously to be a major adhesin of *A. fumigatus* with many functions associated to the invasion of the host tissue (Gresnigt *et al.*, 2014; Robinet *et al.*, 2014). The current study also demonstrated that the production of GAG is increased in response to bacterial assault against the fungus.

Interestingly, the bacteria bind to the fungus principally at the apex that is at the site of the metabolic fungal activity. Increased fixation at the tip of *A. fumigatus* hyphae, where intense production of exudates takes place (Toljander *et al.*, 2007), may be a reason for *P. aeruginosa* to obtain nutrients from the fungus. Similarly, *P. aeruginosa* binding to the hyphal (but not to the yeast) form of *Candida albicans* suggests an interaction via hyphal specific glycoproteins, lectins or adhesins (Hogan and Kolter, 2002). The ligand has not been identified yet.

The present and previous studies from our laboratory and others showed that *P. aeruginosa* produces two types of molecules which can influence *A. fumigatus* growth. The first ones are the toxins which directly kill *A. fumigatus*. Examples of those are phenazines and homoserine lactones (Mowat *et al.*, 2010; Moree *et al.*, 2012; Briard *et al.*, 2015), which display different toxic effects. Phenazines kill the fungus by inducing intracellular reactive-oxygen species and reactive-nitrogen species production (Briard *et al.*, 2015). Homoserine lactones repressed *C. albicans* filamentation (Hogan *et al.*, 2004) and reduced *A. fumigatus* growth, but their mode of action is not yet studied (Mowat *et al.*, 2010).

The second type of compounds is stress molecules which induces a typical anti-stress response from *A. fumigatus*. An example is the diRhls. *A. fumigatus* responds to diRhls in a way which is very similar to any response to environmental molecules including antifungals targeting cell wall such as echinocandins, calcofluor white or congo red (Ram and Klis, 2006; Perlin, 2011; Lee *et al.*, 2012). Interestingly, use of diRhls led to the discovery of a new cell wall compensatory mechanism not previously described, which is the melanin synthesis.

Melanin synthesis is associated with reduced fungal susceptibility to a variety of aggressions. Infection increases the expression of melanin synthesis genes by various fungi and the more virulent strains produce the more melanin (Eisenman and Casadevall, 2012). In the host, melanin interferes with the normal function of phagocytic cells and scavenges reactive-oxygen species (Eisenman and Casadevall, 2012; Chamilos *et al.*, 2016). In *A. fumigatus*, melanin production has been described in biofilm (Beauvais *et al.*, 2007) or *in vivo* the production of DHN-melanin was suggested during experimental aspergillosis under conditions which can be considered to be starved stress conditions (Langfelder *et al.*, 2001). The origin of melanin in *A. fumigatus* biofilm is still unknown. It was hypothesized that melanin resulted from air-oxidation of melanin precursors in the biofilm channels. The use of two *A. fumigatus* mutants unable to produce DHN- and pyo-melanin when co-cultured with *P. aeruginosa* indicated that ECM synthesized by parental *A. fumigatus* in presence of *P. aeruginosa* is composed of DHN- and pyo-melanin (Figure 3). Interestingly the melanin produced by the fungus in response to PAO1 disappeared at the contact region with the bacterium. *Klebsiella aerogenes* synthesizes a dopamine precursor from L-tyrosine that was used by *Cryptococcus neoformans* for melanin production, which required a fungal laccase (Frases *et al.*, 2006). *A. fumigatus* expressed laccases during vegetative growth and a 4-hydroxyphenylpyruvate dioxygenase (HppD) responsible for the synthesis of pyo-melanin from L-tyrosine present in different media (Sugareva *et al.*, 2006; Schmaler-Ripcke *et al.*, 2009). Moreover,

*A. fumigatus* interacting with *P. aeruginosa* Δ*rhlA*, which does not produce any Rhl, did not synthesize melanin demonstrating that the diRhls were inducing the synthesis of the melanin protecting layer by the fungus. However, the antibacterial function of the fungal melanin and especially the role of the two different melanins have not been investigated.

In *P. aeruginosa*, because of their metabolic synthesis, Rhls are usually produced as a mixture of homologs di- and mono-Rhls diverging in terms of lipid chain length. To our knowledge, diRha-$C_{10}$-$C_{10}$ is always the major component (Abalos *et al.*, 2001; Sha *et al.*, 2012; Christova *et al.*, 2013; Singh *et al.*, 2013; Gogoi *et al.*, 2016). DiRha-$C_{10}$-$C_{10}$ showed higher antifungal activities on plant pathogens such as *Penicillium juniculosum* and *Bothytis cinerea* than Rhls (Sha *et al.*, 2012). DiRha-$C_{10}$-$C_{10}$ was also active against *C. albicans* with a MIC > 0,15 mM (Singh *et al.*, 2013). At 7 mM, diRha-$C_{10}$-$C_{10}$ disrupted the biofilms and their biosurfactant activity inhibited cell adhesion. The presence of diRhls after 24 h in PAO1 CF is in accordance with the kinetics of Rhls synthesis by *P. aeruginosa* after the growth ceased (24–96 h) (Haba *et al.*, 2003; Laabei *et al.*, 2014; Schmidberger *et al.*, 2014). Rhamnolipids are overproduced *in vitro* by *P. aeruginosa* during nutrient limitation such as in iron starvation (Schmidberger *et al.*, 2014). *In vivo* in the host, iron concentration is limited, and 2.4–15.3 μg ml$^{-1}$ Rhls were found in sputa of all cystic fibrosis patients chronically infected by *P. aeruginosa* (Kownatzki *et al.*, 1987). Mucoid isolates from chronically infected patients produced more Rhls than non-mucoid isolates (Bjarnsholt *et al.*, 2010). Indeed, they are components of *P. aeruginosa* biofilm and protect the bacteria against phagocytosis by polymorphonuclear neutrophils by inducing necrosis of the latter (Van Gennip *et al.*, 2009).

Until now the effect of all Rhls, including diRha-$C_{10}$-$C_{10}$ and its homologs, was attributed only to their biosurfactant activity, which destabilizes plasma membrane resulting to quantitative changes in phospholipid headgroup (Sha *et al.*, 2012; Sotirova *et al.*, 2012; Singh *et al.*, 2013). Similarly to the role of dihydromaltophilin on plasma membrane sphingolipid biosynthesis (Li *et al.*, 2009), the disorganization of the plasma membrane by diRhls may stimulate cell wall synthesis by activating cell wall integrity signaling pathways, which could explain the thickening of the cell wall. The combination of the rhamnobiose moiety and of the branched aglycon in the diRhls is essential for the interaction with the GS since neither rhamnobiose nor diRha-$C_3$ and diRha-$C_8$ analogs showed an inhibitory activity. Similar inhibition of the GS and growth phenotype in *A. fumigatus* has been observed using echinocandins, such as caspofungin, micofungin or anidulafungin, which are lipopeptides differentiated by their aliphatic tails (Perlin, 2011; Clavaud *et al.*, 2012). Enzymatic removal of the aliphatic tails of the drugs renders them inactive (Perlin, 2011). The antagonistic effect of caspofungin and F-diRhls on *A. fumigatus* confirmed that both lipid conjugates had GS as target. It has been speculated that the tail of the drugs may intercalate into the bilayer resulting in inhibition. Such drug–target interactions would not require the drugs to enter the cell and they may act on the enzyme from the extracellular face of the cell membrane. At the same time, the fact that echinocandin-resistant strain (EMFR S678P) showed high susceptibility to F-diRhls suggested that the inhibitory binding site of F-diRhls differs from that of echinocandin and that the S678P mutation enhances the affinity of F-diRhls for GS. In contrast, the combination of azoles and F-diRhls on *A. fumigatus* was synergic as it was found previously for azoles and echinocandins, which have different inhibitory binding sites (Mavridou *et al.*, 2015).

Other studies showed that *in vitro P. aeruginosa* inhibited the growth of *A. fumigatus*, the cystic fibrosis isolates being more inhibitory than non-cystic fibrosis isolates (Ferreira *et al.*, 2015). Moreover, until now it is not known how *A. fumigatus* colonized better in the respiratory tract of cystic fibrosis patients when they got an infection with *P. aeruginosa* and whether the fungus is in close contact with the bacteria. We showed previously that at low '*in vivo*' concentrations, phenazines stimulated the growth of *A. fumigatus* by providing iron uptake (Briard *et al.*, 2015). It is particularly conceivable that *in vivo A. fumigatus* establishes in the same niches as *P. aeruginosa* taking advantage of favorable growth conditions due to lung damages. *A. fumigatus* may also benefit from the *P. aeruginosa* biofilm for host immune protection due to the role of Rhls and alginate in the reduction of the host immune responses (Baxter *et al.*, 2013; Briard *et al.*, 2015). Moreover, recent studies from our group also showed that these interactions can be observed at distance. Fungi and bacteria do not have to be in contact and volatiles from *P. aeruginosa* can be used as nutrients by the fungus (Briard *et al.*, 2016). These recent data point out the need to investigate in depth the pulmonary microbiota and the cross-talks between bacteria and fungi. In cystic fibrosis patients, the microbiota is completely disorganized and becomes particularly rich in the pathogenic bacteria *P. aeruginosa* and *A. fumigatus* (Delhaes *et al.*, 2012; Baxter *et al.*, 2013; Armstead *et al.*, 2014). Equilibrium in the different partners of the microbiota may be important to avoid allergic bronchopulmonary aspergillosis, *A. fumigatus* bronchitis and other allergic manifestations as well as controlling cystic fibrosis infections and chronic obstructive pulmonary disorders (Whiteson *et al.*, 2014).

## Conflict of Interest

The authors declare no conflict of interest.

# Acknowledgements

# References

Abalos A, Pinazo A, Infante MR, Casals M, García F, Manresa A. (2001). Physicochemical and antimicrobial properties of new rhamnolipids produced by *Pseudomonas aeruginosa* AT10 from soybean oil refinery wastes. *Langmuir* **17**: 1367–1371.

Abdel-Mawgoud AM, Lépine F, Déziel E. (2010). Rhamnolipids: diversity of structures, microbial origins and roles. *Appl Microbiol Biotechnol* **86**: 1323–1336.

Arikan S, Lozano-Chiu M, Paetznick V, Rex JH. (2002). *In vitro* synergy of caspofungin and amphotericin B against *Aspergillus* and *Fusarium* spp. *Antimicrob Agents Chemother* **46**: 245–247.

Armstead J, Morris J, Denning DW. (2014). Multi-country estimate of different manifestations of aspergillosis in cystic fibrosis. *PloS One* **9**: e98502.

Arutchelvi J, Doble M. (2010). Characterization of glycolipid biosurfactant from *Pseudomonas aeruginosa* CPCL isolated from petroleum-contaminated soil. *Lett Appl Microbiol* **51**: 75–82.

Bamford NC, Snarr BD, Gravelat FN, Little DJ, Lee MJ, Zacharias CA *et al.* (2015). Sph3 Is a glycoside hydrolase required for the biosynthesis of galactosaminogalactan in *Aspergillus fumigatus*. *J Biol Chem* **290**: 27438–27450.

Baxter CG, Rautemaa R, Jones AM, Webb AK, Bull M, Mahenthiralingam E *et al.* (2013). Intravenous antibiotics reduce the presence of *Aspergillus* in adult cystic fibrosis sputum. *Thorax* **68**: 652–657.

Beauvais A, Schmidt C, Guadagnini S, Roux P, Perret E, Henry C *et al.* (2007). An extracellular matrix glues together the aerial-grown hyphae of *Aspergillus fumigatus*. *Cell Microbiol* **9**: 1588–1600.

Bjarnsholt T, Jensen PØ, Jakobsen TH, Phipps R, Nielsen AK, Rybtke MT *et al.* (2010). Quorum sensing and virulence of Pseudomonas aeruginosa during lung infection of cystic fibrosis patients. *PloS One* **5**: e10115.

Blyth W. (1971). Modifications in the ultrastructure of *Aspergillus fumigatus* due to the presence of living cells of *Pseudomonas aeruginosa*. *Sabouraudia* **9**: 283–286.

Briard B, Bomme P, Lechner BE, Mislin GLA, Lair V, Prévost M-C *et al.* (2015). *Pseudomonas aeruginosa* manipulates redox and iron homeostasis of its microbiota partner *Aspergillus fumigatus* via phenazines. *Sci Rep* **5**: 8220.

Briard B, Heddergott C, Latgé J-P. (2016). Volatile compounds emitted by *Pseudomonas aeruginosa* stimulate growth of the fungal pathogen *Aspergillus fumigatus*. *mBio* **7**: e00219.

Chamilos G, Akoumianaki T, Kyrmizi I, Brakhage A, Beauvais A, Latge J-P. (2016). Melanin targets LC3-associated phagocytosis (LAP): a novel pathogenetic mechanism in fungal disease. *Autophagy* **12**: 888–889.

Christova N, Tuleva B, Kril A, Georgieva M, Konstantinov S, Terziyski I *et al.* (2013). Chemical structure and in vitro antitumor activity of rhamnolipids from *Pseudomonas aeruginosa* BN10. *Appl Biochem Biotechnol* **170**: 676–689.

Clavaud C, Beauvais A, Barbin L, Munier-Lehmann H, Latgé J-P. (2012). The composition of the culture medium influences the β-1,3-glucan metabolism of Aspergillus fumigatus and the antifungal activity of inhibitors of β-1,3-glucan synthesis. *Antimicrob Agents Chemother* **56**: 3428–3431.

Delhaes L, Monchy S, Fréalle E, Hubans C, Salleron J, Leroy S *et al.* (2012). The airway microbiota in cystic fibrosis: a complex fungal and bacterial community–implications for therapeutic management. *PloS One* **7**: e36313.

Diggle SP, Winzer K, Chhabra SR, Worrall KE, Cámara M, Williams P. (2003). The *Pseudomonas aeruginosa* quinolone signal molecule overcomes the cell density-dependency of the quorum sensing hierarchy, regulates rhl-dependent genes at the onset of stationary phase and can be produced in the absence of LasR. *Mol Microbiol* **50**: 29–43.

Eisenman HC, Casadevall A. (2012). Synthesis and assembly of fungal melanin. *Appl Microbiol Biotechnol* **93**: 931–940.

Elefanti A, Mouton JW, Verweij PE, Tsakris A, Zerva L, Meletiadis J. (2013). Amphotericin B- and voriconazole-echinocandin combinations against *Aspergillus* spp.: effect of serum on inhibitory and fungicidal interactions. *Antimicrob Agents Chemother* **57**: 4656–4663.

Ferreira JAG, Penner JC, Moss RB, Haagensen JAJ, Clemons KV, Spormann AM *et al.* (2015). Inhibition of *Aspergillus fumigatus* and its biofilm by *Pseudomonas aeruginosa* is dependent on the source, phenotype and growth conditions of the bacterium. *PloS One* **10**: e0134692.

Frases S, Chaskes S, Dadachova E, Casadevall A. (2006). Induction by *Klebsiella aerogenes* of a melanin-like pigment in *Cryptococcus neoformans*. *Appl Environ Microbiol* **72**: 1542–1550.

Gogoi D, Bhagowati P, Gogoi P, Bordoloi NK, Rafay A, Dolui SK *et al.* (2016). Structural and physico-chemical characterization of a dirhamnolipid biosurfactant purified from *Pseudomonas aeruginosa*: application of crude biosurfactant in enhanced oil recovery. *RSC Adv* **6**: 70669–70681.

Gresnigt MS, Bozza S, Becker KL, Joosten LAB, Abdollahi-Roodsaz S, van der Berg WB *et al.* (2014). A polysaccharide virulence factor from *Aspergillus fumigatus* elicits anti-inflammatory effects through induction of Interleukin-1 receptor antagonist. *PLoS Pathog* **10**: e1003936.

Haba E, Pinazo A, Jauregui O, Espuny MJ, Infante MR, Manresa A. (2003). Physicochemical characterization and antimicrobial properties of rhamnolipids produced by *Pseudomonas aeruginosa* 47T2 NCBIM 40044. *Biotechnol Bioeng* **81**: 316–322.

Hill D, Rose B, Pajkos A, Robinson M, Bye P, Bell S *et al.* (2005). Antibiotic susceptibilities of *Pseudomonas aeruginosa* isolates derived from patients with cystic fibrosis under aerobic, anaerobic, and biofilm conditions. *J Clin Microbiol* **43**: 5085–5090.

Hogan DA, Kolter R. (2002). *Pseudomonas-Candida* interactions: an ecological role for virulence factors. *Science* **296**: 2229–2232.

1590

Hogan DA, Vik A, Kolter R. (2004). A *Pseudomonas aeruginosa* quorum-sensing molecule influences *Candida albicans* morphology. *Mol Microbiol* **54**: 1212–1223.

Holloway BW, Römling U, Tümmler B. (1994). Genomic mapping of *Pseudomonas aeruginosa* PAO. *Microbiol Read Engl* **140**: 2907–2929.

Jahn B, Boukhallouk F, Lotz J, Langfelder K, Wanner G, Brakhage AA. (2000). Interaction of human phagocytes with pigmentless *Aspergillus conidia*. *Infect Immun* **68**: 3736–3739.

Jensen PØ, Bjarnsholt T, Phipps R, Rasmussen TB, Calum H, Christoffersen L *et al.* (2007). Rapid necrotic killing of polymorphonuclear leukocytes is caused by quorum-sensing-controlled production of rhamnolipid by *Pseudomonas aeruginosa*. *Microbiology* **153**: 1329–1338.

Knutsen AP, Bush RK, Demain JG, Denning DW, Dixit A, Fairs A *et al.* (2012). Fungi and allergic lower respiratory tract diseases. *J Allergy Clin Immunol* **129**: 280–291-293.

Kownatzki R, Tümmler B, Döring G. (1987). Rhamnolipid of *Pseudomonas aeruginosa* in sputum of cystic fibrosis patients. *Lancet* **1**: 1026–1027.

Laabei M, Jamieson WD, Lewis SE, Diggle SP, Jenkins ATA. (2014). A new assay for rhamnolipid detection-important virulence factors of *Pseudomonas aeruginosa*. *Appl Microbiol Biotechnol* **98**: 7199–7209.

Lamarre C, Beau R, Balloy V, Fontaine T, Wong Sak Hoi J, Guadagnini S *et al.* (2009). Galactofuranose attenuates cellular adhesion of *Aspergillus fumigatus*. *Cell Microbiol* **11**: 1612–1623.

Langfelder K, Philippe B, Jahn B, Latgé JP, Brakhage AA. (2001). Differential expression of the *Aspergillus fumigatus* pksP gene detected *in vitro* and *in vivo* with green fluorescent protein. *Infect Immun* **69**: 6411–6418.

Latgé J-P. (2010). Tasting the fungal cell wall. *Cell Microbiol* **12**: 863–872.

Lee KK, Maccallum DM, Jacobsen MD, Walker LA, Odds FC, Gow NAR *et al.* (2012). Elevated cell wall chitin in *Candida albicans* confers echinocandin resistance in vivo. *Antimicrob Agents Chemother* **56**: 208–217.

Li S, Calvo AM, Yuen GY, Du L, Harris SD. (2009). Induction of cell wall thickening by the antifungal compound dihydromaltophilin disrupts fungal growth and is mediated by sphingolipid biosynthesis. *J Eukaryot Microbiol* **56**: 182–187.

Mavridou E, Meletiadis J, Rijs A, Mouton JW, Verweij PE. (2015). The strength of synergistic interaction between posaconazole and caspofungin depends on the underlying azole resistance mechanism of *Aspergillus fumigatus*. *Antimicrob Agents Chemother* **59**: 1738–1744.

Moree WJ, Phelan VV, Wu C-H, Bandeira N, Cornett DS, Duggan BM *et al.* (2012). Interkingdom metabolic transformations captured by microbial imaging mass spectrometry. *Proc Natl Acad Sci USA* **109**: 13811–13816.

Mowat E, Rajendran R, Williams C, McCulloch E, Jones B, Lang S *et al.* (2010). Pseudomonas aeruginosa and their small diffusible extracellular molecules inhibit *Aspergillus fumigatus* biofilm formation. *FEMS Microbiol Lett* **313**: 96–102.

Paugam A, Baixench M-T, Demazes-Dufeu N, Burgel P-R, Sauter E, Kanaan R *et al.* (2010). Characteristics and consequences of airway colonization by filamentous fungi in 201 adult patients with cystic fibrosis in France. *Med Mycol* **48**: S32–S36.

Perlin DS. (2011). Current perspectives on echinocandin class drugs. *Future Microbiol* **6**: 441–457.

Ram AFJ, Klis FM. (2006). Identification of fungal cell wall mutants using susceptibility assays based on Calcofluor white and Congo red. *Nat Protoc* **1**: 2253–2256.

Robinet P, Baychelier F, Fontaine T, Picard C, Debré P, Vieillard V *et al.* (2014). A polysaccharide virulence factor of a human fungal pathogen induces neutrophil apoptosis via NK cells. *J Immunol* **192**: 5332–5342.

Rocha EMF, Garcia-Effron G, Park S, Perlin DS. (2007). A Ser678Pro substitution in Fks1p confers resistance to echinocandin drugs in *Aspergillus fumigatus*. *Antimicrob Agents Chemother* **51**: 4174–4176.

Schmaler-Ripcke J, Sugareva V, Gebhardt P, Winkler R, Kniemeyer O, Heinekamp T *et al.* (2009). Production of pyomelanin, a second type of melanin, via the tyrosine degradation pathway in *Aspergillus fumigatus*. *Appl Environ Microbiol* **75**: 493–503.

Schneider CA, Rasband WS, Eliceiri KW. (2012). NIH Image to ImageJ: 25 years of image analysis. *Nat Met* **9**: 671–675.

Schmidberger A, Henkel M, Hausmann R, Schwartz T. (2014). Influence of ferric iron on gene expression and rhamnolipid synthesis during batch cultivation of *Pseudomonas aeruginosa* PAO1. *Appl Microbiol Biotechnol* **98**: 6725–6737.

Sha R, Jiang L, Meng Q, Zhang G, Song Z. (2012). Producing cell-free culture broth of rhamnolipids as a cost-effective fungicide against plant pathogens. *J Basic Microbiol* **52**: 458–466.

Sharma A, Jansen R, Nimtz M, Johri BN, Wray V. (2007). Rhamnolipids from the rhizosphere bacterium Pseudomonas sp. GRP(3) that reduces damping-off disease in Chilli and tomato nurseries. *J Nat Prod* **70**: 941–947.

da Silva Ferreira ME, Kress MRVZ, Savoldi M, Goldman MHS, Härtl A, Heinekamp T *et al.* (2006). The akuB(KU80) mutant deficient for nonhomologous end joining is a powerful tool for analyzing pathogenicity in *Aspergillus fumigatus*. *Eukaryot Cell* **5**: 207–211.

Singh N, Pemmaraju SC, Pruthi PA, Cameotra SS, Pruthi V. (2013). Candida biofilm disrupting ability of di-rhamnolipid (RL-2) produced from *Pseudomonas aeruginosa* DSVP20. *Appl Biochem Biotechnol* **169**: 2374–2391.

Sotirova A, Avramova T, Stoitsova S, Lazarkevich I, Lubenets V, Karpenko E *et al.* (2012). The importance of rhamnolipid-biosurfactant-induced changes in bacterial membrane lipids of Bacillus subtilis for the antimicrobial activity of thiosulfonates. *Curr Microbiol* **65**: 534–541.

Sugareva V, Härtl A, Brock M, Hübner K, Rohde M, Heinekamp T *et al.* (2006). Characterisation of the laccase-encoding gene abr2 of the dihydroxynaphthalene-like melanin gene cluster of *Aspergillus fumigatus*. *Arch Microbiol* **186**: 345–355.

Toljander JF, Lindahl BD, Paul LR, Elfstrand M, Finlay RD. (2007). Influence of arbuscular mycorrhizal mycelial exudates on soil bacterial growth and community structure. *FEMS Microbiol Ecol* **61**: 295–304.

Van Gennip M, Christensen LD, Alhede M, Phipps R, Jensen PØ, Christophersen L *et al.* (2009). Inactivation of the rhlA gene in *Pseudomonas aeruginosa* prevents

rhamnolipid production, disabling the protection against polymorphonuclear leukocytes. *APMIS Acta Pathol Microbiol Immunol Scand* **117**: 537–546.

Walker LA, Gow NAR, Munro CA. (2010). Fungal echinocandin resistance. *Fungal Genet Biol* **47**: 117–126.

Whiteson KL, Bailey B, Bergkessel M, Conrad D, Delhaes L, Felts B *et al.* (2014). The upper respiratory tract as a microbial source for pulmonary infections in cystic fibrosis. Parallels from island biogeography. *Am J Respir Crit Care Med* **189**: 1309–1315.

Wilson R, Sykes DA, Watson D, Rutman A, Taylor GW, Cole PJ. (1988). Measurement of *Pseudomonas aeruginosa* phenazine pigments in sputum and assessment of their contribution to sputum sol toxicity for respiratory epithelium. *Infect Immun* **56**: 2515–2517.

Supplementary Information accompanies this paper on The ISME Journal website (http://www.nature.com/ismej)